

Research Article

Design of a Noncircular Planetary Gear Mechanism for Hydraulic Motor

Dawei Li ¹, Yongping Liu,¹ Jun Gong ¹ and Tongcheng Wang²

¹School of Mechanical and Electrical Engineering, Lanzhou University of Technology, Lanzhou 730050, China

²Beijing Tianma Electro Hydraulic Control System Company, Ltd., Beijing 100083, China

Correspondence should be addressed to Jun Gong; lut20108020@126.com

Received 11 January 2021; Revised 7 March 2021; Accepted 30 March 2021; Published 10 April 2021

Academic Editor: Nikunja Mohan Modak

Copyright © 2021 Dawei Li et al. This is an open access article distributed under the Creative Commons Attribution License, which permits unrestricted use, distribution, and reproduction in any medium, provided the original work is properly cited.

Given the design difficulty and poor accuracy of tooth profile of noncircular gear used in noncircular gear hydraulic motor, it is proposed to reduce the design difficulty and improve the design accuracy by using arc-shaped pitch curve instead of noncircular pitch curve with continuously varying curvature. Based on the geometric relationship and transmission relationship of the noncircular planetary gear mechanism, a nonlinear programming model is constructed for the circular arc-shaped pitch curve. By solving the nonlinear programming model, a noncircular planetary gear mechanism with a modulus of $m = 1.5$ is designed. The noncircular gear mechanism with the arc-shaped pitch curve was machined and installed in a hydraulic motor, and an efficiency comparison experiment was conducted with a high-order elliptical noncircular gear mechanism with a continuously varying curvature. The experiment shows that the efficiency of the two noncircular gear mechanisms is basically the same, and the best speed range is 100–400 rpm. The noncircular planetary gear mechanism with an arc-shaped pitch curve designed in this paper has reasonable structure, correct transmission relationship, and simple design method, which shows that the design method proposed in this paper has a good engineering application value.

1. Introduction

The noncircular gear mechanism has a compact structure and high transmission torque and is widely used in various machines, such as seedling pick-up mechanism for vegetable [1], transplanting mechanism for rice [2], gravity equilibrators [3], bucket wheel stacker [4], and differential velocity vane pump [5]. The noncircular gear hydraulic motor with the noncircular gear mechanism as the core component has a small size, high torque, and smooth transmission and can use a nonflammable emulsion as the working medium, which can improve the safety factor when used in a high gas environment such as a mine and therefore has good application prospects.

The first generation of noncircular planetary gear hydraulic motor was invented by Bohdan Sieniawski [6] back in 1977. Some researchers have also researched the design and application of this type of motor [7, 8]. With the development of computer technology, the geometry of

noncircular gears in such motors is not only limited to third-order elliptical, and more complex noncircular gear mechanisms with better performance have appeared. In conclusion, the design of different structural types of noncircular gears is the key to designing a noncircular gear hydraulic motor with excellent performance.

About noncircular gears, Lin et al. [9–12] studied the contact characteristics, kinematic characteristics, and load characteristics of noncircular gears, which laid a solid foundation for the popularization of noncircular gears. Han [13–15] studied the design method of noncircular gear tooth profile and established a multiaxis linkage model of CNC hobbing to realize digital manufacturing of noncircular gears. Xu [16] studied the design method of noncircular gear vice, which can design the noncircular gear pitch curve with its conjugate as well as the tooth profile. Lyashkov [17] established an automated model for the geometric design of noncircular gears, using multisegment arcs instead of complex tooth profile curves to shorten the design cycle of

noncircular gears. Many researchers have made substantial contributions to the study of design methods for noncircular gears [18–20]. Sclater [21] shows many mechanical drives, including planetary gear systems based on noncylindrical gears, further expanding the field of application of noncylindrical gears.

Although a lot of researchers have studied noncircular gears, the design of a noncircular gear tooth profile is still complicated and difficult because the pitch curve of noncircular gears has continuously varying curvature, which brings great inconvenience to the promotion and use of such noncircular gear hydraulic motor. Moreover, for the noncircular gears in such a hydraulic motor, no pitch curve equation can be expressed by a unified independent variable, and the geometric model of the pitch curve can only be constructed with discrete data points in the design, which is not only a large workload but also difficult to ensure the required design accuracy. In contrast, the tooth profile design method of cylindrical gears is simple and the design cycle is short. If the pitch curve of noncircular gears can be designed as arc, the tooth profile of a certain circular gear can be used instead of the tooth profile of noncircular gears in a certain arc segment, thus reducing the difficulty of designing the tooth profile of noncircular gears.

In a noncircular planetary gear mechanism, the geometry of the center wheel and the inner gear ring and their transmission relations with the planetary wheel should satisfy certain constraints, which may be more complex nonlinear relations [22–25]. Therefore, a nonlinear programming model of the arc-shaped pitch curve can be constructed to obtain a noncircular planetary gear mechanism that satisfies the transmission relationship.

The purpose of this paper is to design a noncircular planetary gear mechanism with a fixed curvature pitch curve to replace the existing noncircular gear mechanism with a continuously varying curvature pitch curve in a hydraulic motor. By replacing the noncircular gear profile with a cylindrical gear profile of the same shape, the design of the noncircular planetary gear mechanism is made less difficult and the newly designed noncylindrical planetary gear mechanism is able to operate normally in the hydraulic motor with efficiency no less than that of the original gear mechanism.

2. The Working Principle of Noncircular Gear Hydraulic Motor and the Pitch Curve of Noncircular Gear

2.1. Working Principle of Noncircular Gear Hydraulic Motor. As shown in Figure 1, the noncircular gear hydraulic motor is mainly composed of a noncircular planetary gear mechanism, flow distribution disc, and other parts. It relies on the center wheel, inner gear ring, and several planetary wheels meshing to form a sealed volume cavity. Under the action of pressure, the volume of the sealed cavity will change, prompting the center wheel to rotate, thus outputting torque and speed. It can be seen that the noncircular gear pitch curve directly determines whether the hydraulic motor can work properly.

2.2. High-Order Elliptic Pitch Curve. The noncircular planetary gear mechanism is the core of a noncircular gear hydraulic motor. The geometry of the noncircular gear pitch curve directly determines whether the planetary gear mechanism can be properly meshed and continuously driven. In the previous noncircular planetary gear mechanism, the pitch curve of noncircular gears is of high-order elliptical type, which can be expressed in polar coordinates as

$$r = \frac{A(1 - k^2)}{1 - k \cos(n\varphi)}, \quad (1)$$

where r is the directional diameter of the pitch curve, φ is the polar angle of the pitch curve, A is the long-axis radius of the ellipse, k is the eccentricity of the ellipse, and n is the order of the ellipse. Taking the ellipse of order 4 as an example, the long-axis radius of the elliptical gear pitch curve with modulus $m = 1.5$ is $A = 32.42$ and the eccentricity is $k = 0.077$ according to the transmission relationship of the noncircular planetary gear mechanism, and the curve is shown in Figure 2.

The elliptical pitch curve has continuously varying curvature, so the adjacent teeth of elliptical gears have different tooth profiles, which not only increases the difficulty of designing but also brings great difficulties to gear processing.

Meanwhile, the pitch curve of the 6th order internal gear ring with the 4th order elliptical gear has no polar equation expressed by a single function and can only be generated using a series of discrete points, which not only consumes a lot of computational resources but also has poor accuracy. The equation for calculating the data points of the pitch curve of the internal gear ring can be expressed as a combination of two equations.

As can be seen, the pitch curve of the internal gear ring is not a continuous curve with a uniform equation. Therefore, the accuracy of the pitch curve of the internal ring depends entirely on the density of the calculated discrete points. To obtain a high-precision pitch curve, more discrete data points need to be calculated, consuming enormous computing resources. It is also necessary to design many individual gear teeth according to the curvature of the pitch curve, which is very unfavorable for engineering applications.

Therefore, by designing knuckle curves with the same curvature, the number of individually designed gear teeth can be reduced, improving design accuracy and reducing the difficulty of design.

2.3. Noncircular Gear Pitch Curves Formed by Circular Arc Curves. A simplified method of noncircular gear design is proposed in this paper, in which several arcs are joined together to form a new pitch curve to replace the original high-order elliptical pitch curve. Taking the most widely used 4–6 noncircular planetary gear mechanism as an example, the arc-shaped pitch curve of the center wheel can be obtained by combining and arraying two arcs of different

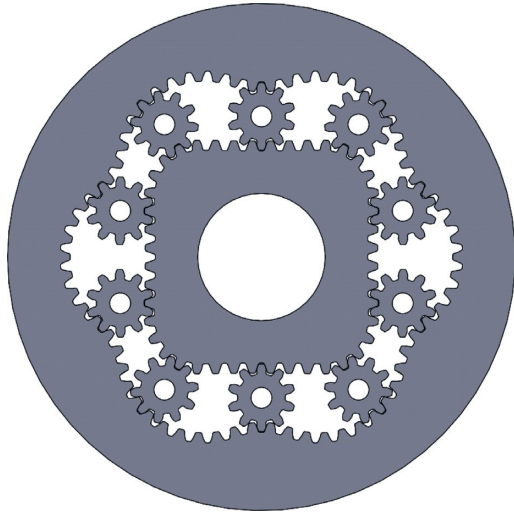


FIGURE 1: Noncircular gear hydraulic motor.

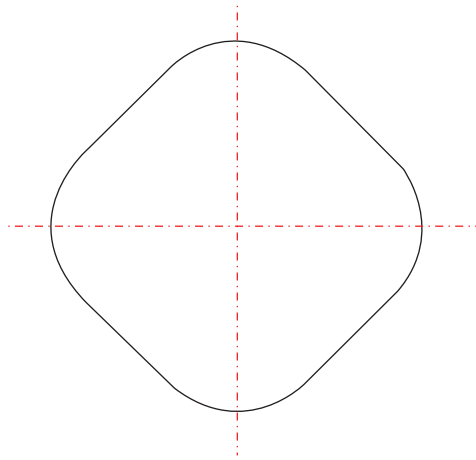


FIGURE 2: High-order elliptic nodal curve.

radius, as shown in Figure 3. The center of the arc \widehat{AB} is O_1 , the distance from the origin is x_1 , and the radius is r_1 . The center of the arc \widehat{CB} is O_{11} , the distance from the origin is y_1 , and the radius is r_{11} . It is only necessary to determine the position of the center of the two segments and the radius of the arc to uniquely determine an arc-shaped pitch curve of noncircular center gear.

Similar to the center wheel, the pitch curve of the inner ring in a noncircular planetary gear mechanism can also be constructed with arcs, as shown in Figure 4. The entire pitch curve can be composed of two segments. The center of the arc \widehat{DE} is O_2 , the distance from the origin is x_2 , and the radius is r_2 . The center of the arc \widehat{FE} is O_{22} , the distance from the origin is y_2 , and the radius is r_{22} .

The radius of curvature of the arc-shaped pitch curve only produces one step at the arc connection point (B, E), and the other stages are circular arcs of equal radius, so the tooth profile of a cylindrical gear can be used instead of the tooth profile of a noncircular gear whose tooth shape varies with the pitch curve. This method can effectively reduce the design difficulty of involute tooth profile as well as manufacturing difficulty and has higher engineering application value.

3. Nonlinear Programming Model for Arc-Shaped Pitch Curves

It is only necessary to determine the radius and the position of the center of the arc to obtain the model of the arc-shaped pitch curve. In planetary gear mechanisms, the geometry of the noncircular gears and their relative position to the central wheel need to satisfy defined constraints, which may be complex nonlinear relationships. Therefore, a nonlinear programming model of the pitch curve is constructed with the radius and center position of the arc as design variables, and a computer is used to help us find the optimal center position and radius of the arc that satisfies the defined constraints.

3.1. Constraints on Nonlinear Programming Models

3.1.1. Conditions for Uniform Distribution of Gear Teeth. To ensure the uniform distribution of the gear teeth on the pitch curve, the arc length of the pitch curve should satisfy the condition of uniform distribution of the gear teeth, which can be expressed as

$$\begin{aligned} L_{\widehat{AB}} + L_{\widehat{CB}} &= \frac{\pi m z_1}{8}, \\ L_{\widehat{DE}} + L_{\widehat{FE}} &= \frac{\pi m z_2}{12}, \end{aligned} \quad (2)$$

where m is the gear module, z_1 and z_2 are the number of teeth of the central wheel and the inner ring, respectively, the number of teeth of the central wheel is preferably 44, and the number of teeth of the inner ring is preferably 66.

3.1.2. Conditions under Which Gears Can Be Continuously Driven. The transmission law of the noncircular planetary gear mechanism should change periodically; therefore, the section curve in one cycle is taken to analyze the transmission relationship of the noncircular gear mechanism. As shown in Figure 5, when the planetary wheel is in the first special meshing position, the maximum diameter of the center wheel pitch curve and the maximum diameter of the internal gear ring pitch curve are in common. The corresponding relationship equation can be expressed as

$$x_1 + r_1 + 2r_3 = x_2 + r_2, \quad (3)$$

where r_3 is the radius of the cylindrical planetary gear.

As shown in Figure 6, when the planetary wheel is in the second special engagement position, the minimum directional diameter of the center wheel and the minimum directional diameter of the inner gear ring are in common line; the corresponding relationship equation can be expressed as

$$y_1 - r_{11} = y_2 - r_{22} - 2r_3. \quad (4)$$

As shown in Figure 7, when the planetary wheel is in the third special engagement position, the planetary wheel engages with the center wheel at point B and with the inner gear ring at point E. In Figure 7, D' is the engagement point of point D on the inner ring and is the engagement point of

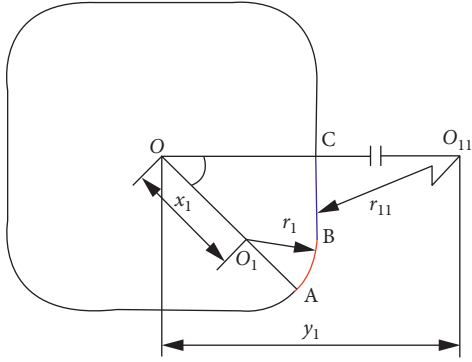


FIGURE 3: Arc-shaped pitch curve of the center gear.

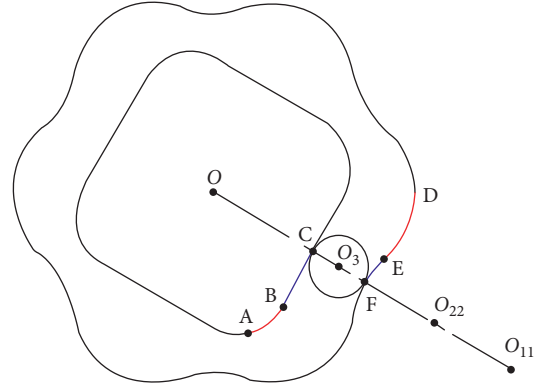


FIGURE 6: The second engagement position.

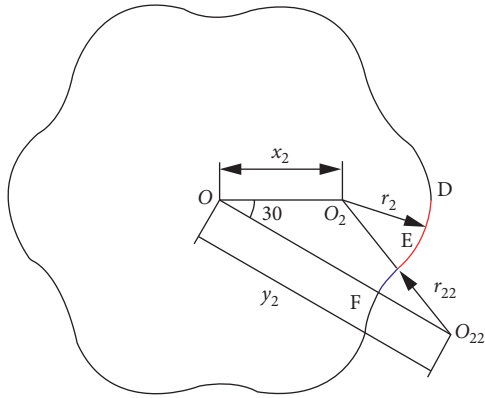


FIGURE 4: Arc-shaped pitch curve of the inner gear ring.

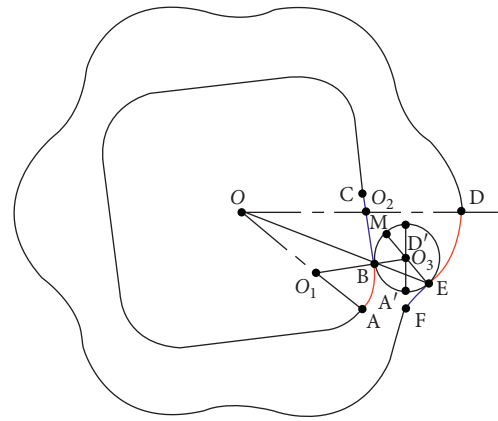


FIGURE 7: The third engagement position.

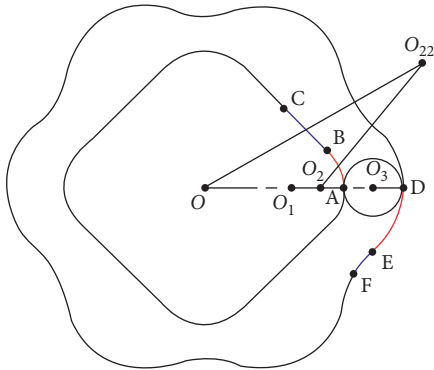


FIGURE 5: The first engagement position.

point A on the central wheel. Since the gears are purely rolling with each other, the corresponding relationship equation can be expressed as

$$L_{DE} = L_{AB} + L_{BM}, \quad (5)$$

where point M is the intersection of the line E-O₃ and the planetary wheel knuckle curve.

3.1.3. Constraints to Avoid Gear Tooth Interference and Undercutting. To avoid interference between the center wheel and the inner ring during rotation, equation (6) should be satisfied. It means that the maximum directional

diameter of the center wheel should be smaller than the minimum directional diameter of the inner ring, and to avoid undercutting, the radius of each segment of the arc should satisfy equation (7):

$$x_1 + r_1 < y_2 - r_{22}, \quad (6)$$

$$r_1, r_{11}, r_2, r_{22} < 5m. \quad (7)$$

3.2. Objective Function on Nonlinear Programming Models. As shown in Figure 7, when the wheel system is in the third special engagement position, the points O₁, B, and O₃ are colinear; a new equation can be obtained as

$$\angle OBO_1 = \angle BEO_3. \quad (8)$$

Therefore, the objective function of the programming model can be constructed using the relation (10). The objective function can be expressed as

$$f = |\angle OBO_1 - \angle BEO_3|, \quad (9)$$

where $\angle OBO_1$ can be expressed by x_1 , y_1 , and r_1 , and $\angle BEO_3$ can be expressed as by x_2 , y_2 , and r_2 . Calculating the minimum value of the objective function shown in equation (9) and ensuring that the design variables satisfy all the constraints, the parameters of the arc-shaped noncircular gear pitch curve can be obtained.

4. Design of Arc-Shaped Pitch Curve

4.1. *Mathematical Expression of the Nonlinear Programming Model for Arc-Shaped Pitch Curves.* Through the above analysis, both the objective function and the arc lengths in each constraint can be expressed as functions with $x_1, y_1, r_1,$

$x_2, y_2,$ and r_2 as independent variables. The mathematical model of the nonlinear programming model can be represented as follows:

The objective function:

$$f(\min) = \left| \arccos \frac{2r_2^2 - r_2(x_2 + z_2^2 - y_2^2/z_2)}{2r_2 \sqrt{x_2^2 + r_2^2 - r_2(x_2 + z_2^2 - y_2^2/z_2)}} - \arccos \frac{2r_1^2 - r_1(x_1 + z_1^2 - y_1^2/z_1)}{2r_1 \sqrt{x_1^2 + r_1^2 - r_1(x_1 + z_1^2 - y_1^2/z_1)}} \right|, \quad (10)$$

s. t.

(1) Conditions for uniform distribution of gear teeth:

$$\begin{aligned} r_1 \left[\pi - \arccos \frac{x_1^2 - x_1 y_1 \cos(\pi/4)}{x_1 z_1} \right] + [z_1 - r_1] \left[\frac{3\pi}{4} - \arccos \frac{x_1^2 - x_1 y_1 \cos(\pi/4)}{x_1 z_1} \right] &= 5.5\pi m, \\ r_2 \left[\pi - \arccos \frac{x_2^2 - x_2 y_2 \cos(\pi/6)}{x_2 z_2} \right] + [z_2 - r_2] \left[\frac{5\pi}{6} - \arccos \frac{x_2^2 - x_2 y_2 \cos(\pi/6)}{x_2 z_2} \right] &= 5.5\pi m. \end{aligned} \quad (11)$$

(2) Conditions under which gears can be continuously driven:

$$\begin{aligned} x_1 + r_1 + 2r_3 &= x_2 + r_2, \\ y_1 - z_1 - r_1 &= y_2 + r_2 - z_2 - 2r_3, \\ r_2 \left[\pi - \arccos \frac{x_2^2 - x_2 y_2 \cos(\pi/6)}{x_2 z_2} \right] &= r_1 \left[\pi - \arccos \frac{x_1^2 - x_1 y_1 \cos(\pi/4)}{x_1 z_1} \right] + 2r_3 \arccos \frac{2r_2^2 - r_2(x_2 + z_2^2 - y_2^2/z_2)}{2r_2 \sqrt{x_2^2 + r_2^2 - r_2(x_2 + z_2^2 - y_2^2/z_2)}}. \end{aligned} \quad (12)$$

(3) Conditions for noninterference between the center wheel and the inner gear ring:

$$x_1 + r_1 < y_2 + r_2 - z_2 \quad (13)$$

(4) Conditions to avoid undercutting:

$$\begin{aligned} r_1 &< 5m, \\ r_2 &< 5m, \\ z_1 - r_1 &< 5m, \\ z_2 - r_2 &< 5m, \end{aligned} \quad (14)$$

where z_1 and z_2 can be expressed as $z_1 = \sqrt{x_1^2 + y_1^2 - 2x_1 y_1 \cos(\pi/4)}$ and $z_2 = \sqrt{x_2^2 + y_2^2 - 2x_2 y_2 \cos(\pi/6)}$.

4.2. *Solution of the Nonlinear Programming Model and Tooth Design.* Take a noncircular planetary gear mechanism with a modulus of $m=1.5$ as an example and solve for the optimized values of the design variables. Assuming that the

result of the calculation is $X = [x_1 \ y_1 \ r_1 \ x_2 \ y_2 \ r_2]$, the lower bound of the solution domain is $[0 \ 0 \ 0 \ 0 \ 0 \ 0]$, the upper bound of the solution domain is $[10^3 \ 10^4 \ 10^3 \ 10^3 \ 10^3 \ 10^3]$, and the initial value of the solution domain is $[10 \ 100 \ 10 \ 10 \ 10 \ 10]$. The final calculation result is $X = [22.29 \ 648.39 \ 12.89 \ 59.22 \ 63.44 \ 20.58]$, and the minimum value of the objective function is 0.0042.

Taking the center wheel as an example, the tooth profile corresponding to the section AC pitch curve is designed as shown in Figure 8. The tooth profiles of other sections can be obtained from the tooth profile array AC.

Since the curvature of the pitch curve steps at point B, the profile of the section AB should be the same as that of the external cylindrical gear with radius r_1 , and the profile of the section CB should be the same as that of the internal cylindrical gear with radius r_{11} . The design parameters of the noncircular planetary gear mechanism are shown in Table 1.

5. Experiment

5.1. *Setup of the Experiment.* The noncircular gear mechanism with the arc-shaped pitch curve was machined by a

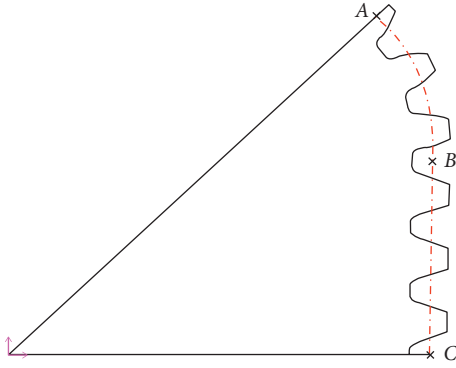


FIGURE 8: Center wheel involute tooth profile.

TABLE 1: The parameters of the noncircular planetary gear mechanism.

	Inner gear ring	Center wheel	Planetary wheel
Modulus (mm)	1.5	1.5	1.5
Number of teeth	66	44	10
Tooth width (mm)	22	22	22
Addendum coefficient	0.8	0.8	0.8
Tip clearance coefficient	0.12	0.12	0.12
Modification coefficient	0	0	-0.103

slow-walking EDM machine and installed in a hydraulic motor with a theoretical displacement of 100 mL/r. The performance was tested and compared with the performance of a noncircular planetary gear hydraulic motor of HPM100, which has a continuously varying curvature of high-order elliptical type. The machined arc-shaped noncircular gear mechanism is shown in Figure 9(a).

The test equipment used is shown in Figure 9(b). The test equipment mainly includes (1) ZJ-1000A torque-speed sensor with rated torque and 4000 rpm permissible speed; (2) FZ1000.J/Y magnetic powder brake with rated torque; (3) TR-3A torque-speed power acquisition instrument. Among them, the load is applied by the magnetic powder brake at the output of the hydraulic motor; the torque-speed sensor is installed on the magnetic powder brake to transmit the torque and speed signals to the power acquisition instrument in real-time. The test working medium is water-based emulsion, HFA98%, and the power is provided by the test base pump station.

The test equipment used is shown in Figure 9(b). The test equipment mainly includes (1) ZJ-1000A torque-speed sensor with a rated torque of 1000N · m and a permitted speed of 4000 rpm. (2) FZ1000.J/Y magnetic powder brake with a rated torque of 1000N · m. (3) TR-3A torque-speed power acquisition instrument. Among them, the load is applied by the magnetic powder brake at the output of the hydraulic motor; the torque-speed sensor is installed on the magnetic powder brake to transmit the torque and speed

signals to the power acquisition instrument in real-time. The test working medium is water-based emulsion, HFA98%, and the power is provided by the test base pump station.

5.2. *Experimental Methods and Results.* Set the initial load torque to 100N · m, accelerate the hydraulic motor to 800 rpm, load the hydraulic motor by magnetic powder brake, and record the speed and torque value until the motor stops due to excessive load torque. The data that can be measured directly during the test include rotational speed, torque, flow rate, and differential pressure.

The motor is stopped before the motor speed falls below 40 rpm. The torque characteristic curve at 50–800 rpm is shown in Figure 10.

The torque characteristic curve shows that the torque of the two hydraulic motors decreases with the increase of the rotational speed. When the speed is less than 400 rpm, the torque of the hydraulic motor installed the noncircular gear mechanism with the arc-shaped pitch curve decreasing slowly with the increase of the speed.

When the rotational speed is higher than 400 rpm, the torque of both hydraulic motors decreases sharply as the rotational speed continues to rise. From the torque characteristics, the best speed range of the newly developed hydraulic motor should be 100–400 rpm.

The same power characteristic curves of the two hydraulic motors can be obtained in the test, as shown in Figure 11.

The power characteristic curve shows that with the increase of speed, the power of both two hydraulic motors increases gradually and then decreases. When the speed is lower than 400 rpm, the power of the motor equipped with the arc-shaped noncircular gear mechanism increases linearly with the speed. It can be seen that this kind of non-circular gear mechanism in use should keep the speed less than 400 rpm which is appropriate.

By using the displacement and pressure, the efficiency can be calculated. The total efficiency curves of the two hydraulic motors are shown in Figure 12.

When the rotational speed is higher than 400 rpm, the efficiency of the two motors decreases sharply with the increase of rotational speed. This is because as the speed increases, the pump station output flow increases, so the total hydraulic power at the input of the motor increases, but when the mechanical power at the output of the hydraulic motor increases to the maximum, the speed continuing to rise will lead to a rapid decline in torque, thus the mechanical power at the output of the motor decreases sharply, so the efficiency of the motor decreases rapidly. When the speed is lower than 300 rpm, the total efficiency of the motor installed with the arc-shaped noncircular gear mechanism is 45.89% at maximum. It has basically the same work efficiency curve as the HPM100 motor, which indicates that the arc-type noncircular planetary gear mechanism designed in this paper has a reasonable structure and similar performance to the traditional high-order elliptical noncircular gear mechanism.

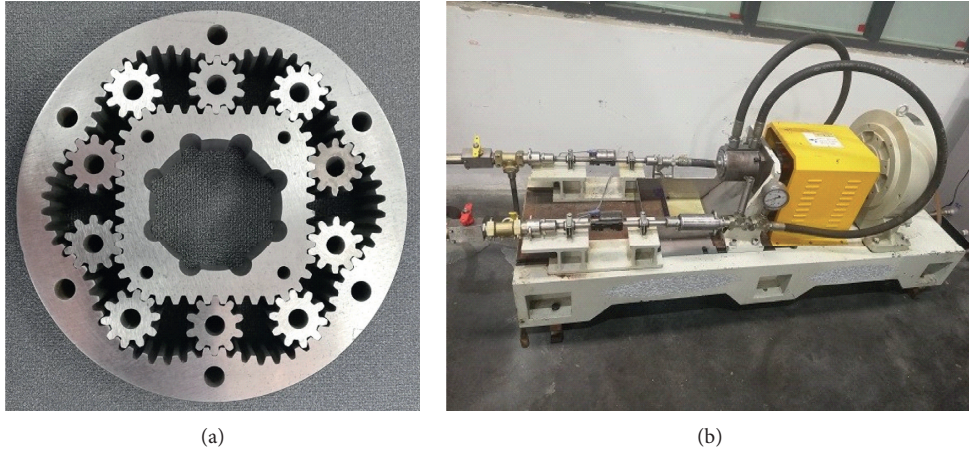


FIGURE 9: (a) Self-made noncircular planetary gear mechanism. (b) Hydraulic motor test device.

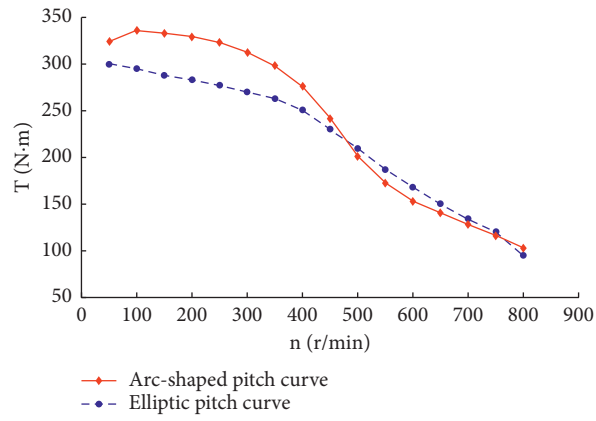


FIGURE 10: Speed-torque characteristic curve.

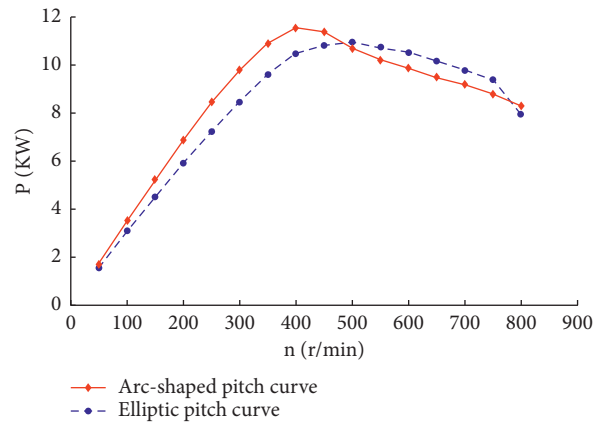


FIGURE 11: Power curve.

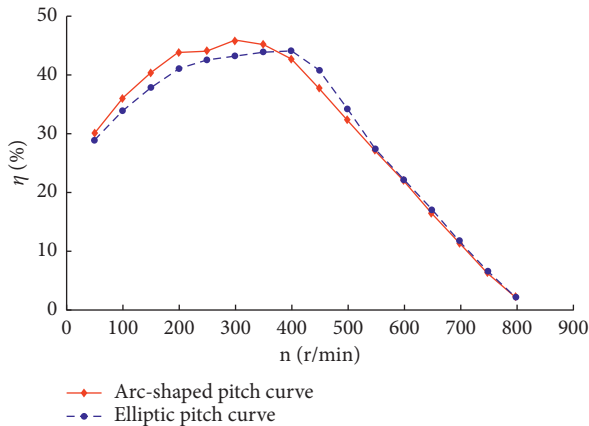


FIGURE 12: Efficiency curve.

6. Conclusions

- (1) The pitch curve of the arc-shaped noncircular planetary gear mechanism is constrained by several nonlinear relations as well as inequality relations; a nonlinear programming model of the pitch curve can be established to solve the modeling parameters of the pitch curve of the arc-shaped noncircular gear mechanism.
- (2) According to the design method proposed in this paper, a noncircular gear mechanism with a displacement of 100 mL/r was machined by EDM wire cutting and installed in the hydraulic motor, and the performance test was conducted under the same conditions as the HPM100 type noncircular gear hydraulic motor. The test results show that when the speed of the hydraulic motor with the arc-shaped noncircular gear mechanism is lower than 400 rpm, the torque decreases slowly as the speed increases, and the hydraulic power increases linearly with the speed, so the optimal speed range of this noncircular gear mechanism should be 100–400 rpm. By comparing the efficiency of the two motors, it can be seen that the working efficiency of the arc-shaped noncircular gear mechanism is basically the same as that of the high-order elliptic noncircular gear mechanism, which indicates that the arc-shaped noncircular gear mechanism designed in this paper has a reasonable structure.
- (3) Because the pitch curve of the original noncircular gear has continuously varying curvature and each tooth has a different tooth profile, it is necessary to design the tooth profile of each tooth individually, which greatly increases the difficulty of designing noncircular gear mechanisms. The arc-shaped pitch curve has the same curvature, so it is possible to use only one tooth profile of a cylindrical gear instead of several noncircular gear profiles, which significantly reduces the number of tooth profiles that need to be designed separately, thus reducing the difficulty of designing noncircular gear mechanisms.

Data Availability

The data used to support the findings of this study are available from the corresponding author upon request.

Conflicts of Interest

The authors declare that they do not have any commercial or associative interest that represents conflicts of interest in connection with the work submitted.

Acknowledgments

This research was supported by the National Natural Science Foundation of China (51765032).

References

- [1] B. Ye, G. J. Zeng, G. Zeng et al., "Design and tests of a rotary plug seedling pick-up mechanism for vegetable automatic transplanter," *International Journal of Agricultural and Biological Engineering*, vol. 13, no. 3, pp. 70–78, 2020.
- [2] X. Zhao, M. Y. Chu, X. X. Ma, L. Dai, B. L. Ye, and J. N. Chen, "Research on design method of non-circular planetary gear train transplanting mechanism based on precise poses and trajectory optimization," *Advances in Mechanical Engineering*, vol. 10, no. 12, p. 12, 2018 Art. no. 1687814018814368.
- [3] B. G. Bijlsma, G. Radaelli, J. L. Herder, and Asme, "Design OF a compact gravity equilibrator with an unlimited range OF motion," in *Proceedings of the Asme International Design Engineering Technical Conferences and Computers and Information in Engineering Conference*, vol. 5aAmer Soc Mechanical Engineers, New York, NY, USA, August 2016.
- [4] Y. L. Yuan, X. G. Song, W. Sun, and X. B. Wang, "Modeling and dynamic analysis of the non-circular gear system of a bucket wheel stacker/reclaimer," *Aip Advances*, vol. 8, no. 6, p. 8, 2018 Art. no. 065318.
- [5] G. Xu, J. Chen, and H. Zhao, "Numerical calculation and experiment of coupled dynamics of the differential velocity vane pump driven by the hybrid higher-order fourier non-circular gears," *Journal of Thermal Science*, vol. 27, no. 3, pp. 285–293, 2018.
- [6] B. Sieniawski, "Gyrating-cam engine, particularly as a hydraulic engine," *U.S. Patent No.* vol. 3, p. 852, 1974.
- [7] Q. Yao and F. Yao, "Planetary rotary type fluid motor or engine and compressor or pump," *U.S. Patent No.* vol. 9, p. 272, 2016.
- [8] S. G. Yang, L. Li, and L. J. Lu, "Static and dynamic characteristics of a novel mine roofbolter driven by non-circular planetary gear hydraulic motor," *Journal of the Chinese Society of Mechanical Engineers*, vol. 36, no. 4, pp. 333–340, 2015.
- [9] C. Lin, C. J. He, and Y. N. Hu, "Analysis on the kinematical characteristics of compound motion curve-face gear pair," *Mechanism and Machine Theory*, vol. 128, pp. 298–313, 2018.
- [10] C. J. He and C. Lin, "Analysis of loaded characteristics of helical curve face gear," *Mechanism and Machine Theory*, vol. 115, pp. 267–282, 2017.
- [11] C. Lin and C. J. He, "Analysis of tooth contact and transmission errors of curve-face gear," *Proceedings of the Institution of Mechanical Engineers Part C-Journal of Mechanical Engineering Science*, vol. 231, no. 19, pp. 3579–3589, 2017.
- [12] C. Lin and X. Wu, "Calculation and characteristic analysis of tooth width of eccentric helical curve-face gear," *Iranian*

- Journal of Science and Technology, Transactions of Mechanical Engineering*, vol. 43, no. 4, pp. 781–797, 2019.
- [13] J. Han, D. Z. Li, L. Xia, X. Q. Tian, and Asme, “Analytical study on tooth profile of non-circular gear based ON hobbing process simulation,” in *Proceedings of the Asme 14th International Manufacturing Science and Engineering Conference*, vol. 2Amer Soc Mechanical Engineers, New York, NY, USA, June 2019.
- [14] J. Han, D. Z. Li, X. Q. Tian, and L. Xia, “Linkage model and interpolation analysis of helical non-circular gear hobbing,” *Journal of the Brazilian Society of Mechanical Sciences and Engineering*, vol. 42, no. 11, p. 13, 2020 Art. no. 582.
- [15] J. Han, Y. Y. Liu, D. Z. Li, and L. Xia, “External high-order multistage modified elliptical helical gears and design procedure of their gear pairs,” *Proceedings of the Institution of Mechanical Engineers Part C-Journal of Mechanical Engineering Science*, vol. 230, no. 16, pp. 2929–2939, 2016.
- [16] H. Xu, T. W. Fu, P. Song, M. J. Zhou, C. W. Fu, and N. J. Mitra, “Computational design and optimization of non-circular gears,” *Computer Graphics Forum, Article; Proceedings Paper*, vol. 39, no. 2, pp. 399–409, 2020.
- [17] A. A. Lyashkov, K. L. Panchuk, and I. A. Khasanova, “Automated geometric and computer-aided non-circular gear formation modeling,” in *Mechanical Science and Technology Update* Vol. 1050, Iop Publishing Ltd, Bristol, UK, 2018.
- [18] F. Zheng, L. Hua, X. Han, B. Li, and D. Chen, “Synthesis of indexing mechanisms with non-circular gears,” *Mechanism and Machine Theory*, vol. 105, pp. 108–128, 2016.
- [19] F. Y. Zheng, X. H. Han, H. Lin, M. D. Zhang, and W. Q. Zhang, “Design and manufacture of new type of non-circular cylindrical gear generated by face-milling method,” *Mechanism and Machine Theory*, vol. 122, pp. 326–346, 2018.
- [20] J. F. Yu, G. L. Ding, and Y. L. Zhang, “Research on the three dimensional modeling method of automobile steering rocker shaft non-circular sector gear,” Edited by M. S. Cao, Ed., in *Proceedings of the 3rd Annual International Conference on Mechanics and Mechanical Engineering*, vol. 105, pp. 1007–1014, Atlantis Press, Sichun, China, December 2017.
- [21] N. Sclater, *Mechanisms and Mechanical Devices Sourcebook*, McGraw-Hill Education, New York, NY, USA, 2011.
- [22] Z. Wang, G. He, W. Du et al., “Application of parameter optimized variational mode decomposition method in fault diagnosis of gearbox,” *IEEE Access*, vol. 7, pp. 44871–44882, 2019.
- [23] Y. Wang, Q. Qian, G. Chen, S. Jin, and Y. Chen, “Multi-objective optimization design of cycloid pin gear planetary reducer,” *Advances in Mechanical Engineering*, vol. 9, no. 9, Art. no. 1687814017720053, 2017.
- [24] X. x. Liu and Q. y. Pan, “Fuzzy multi-object optimization design of helical gear drive,” Edited by M. R. Said, L. Lu, and N. AbuBakar, Eds., in *Proceedings of the 2017 International Conference on Manufacturing Engineering and Intelligent Materials*, vol. 100, pp. 45–49, 2017.
- [25] K. Huang, J. Ma, G. Xia, Z. Zhou, and Z. Zhang, “Interval multi-objective optimization for the specific power of a helicopter’s main reducer planetary gear trains,” *Journal of Aerospace Power*, vol. 32, no. 10, pp. 2447–2455, 2017.